A MODEL OF EDDY-CURRENT PROBES WITH FERRITE CORES*

Harold A. Sabbagh

Analytics, Inc.
2634 Round Hill Lane
Bloomington, IN 47401

INTRODUCTION

The classical work of Dodd and his coworkers at the Oak Ridge National Laboratory deals with the analysis, design and optimization of eddy-current probe coils wound around an air core. Many applications, however, require that the magnetic field produced by the probe coil be "shaped" or confined to certain regions of space, especially at higher frequencies, and this necessitates the use of highly permeable core materials, such as ferrites.

The problem we propose to solve is depicted in Figure 1. It consists of an arbitrarily shaped body-of-revolution made of a ferrite (or other highly permeable material), excited by a coaxial coil, and in the presence of a plane-parallel stratified half-space of conducting materials. The half-space simulates the workpiece, in eddy-current nondestructive evaluation (NDE) parlance. As Figure 1 indicates, the system, composed of the core, coil and half-space, is axisymmetric; this is the simplest, realistic, three-dimensional problem of any degree of generality.

Though the model that we will develop is applicable to arbitrarily shaped bodies-of-revolution, we will specifically attack the problems posed by the core shapes of Figures 2 and 3. The E-shaped core of Figure 2 is typically used in low-frequency eddy-current

*This work was supported by the Naval Surface Weapons Center (Code R34), White Oak Labs, Silver Spring, MD 20910, under Contract No. N60921-81-C-0076.

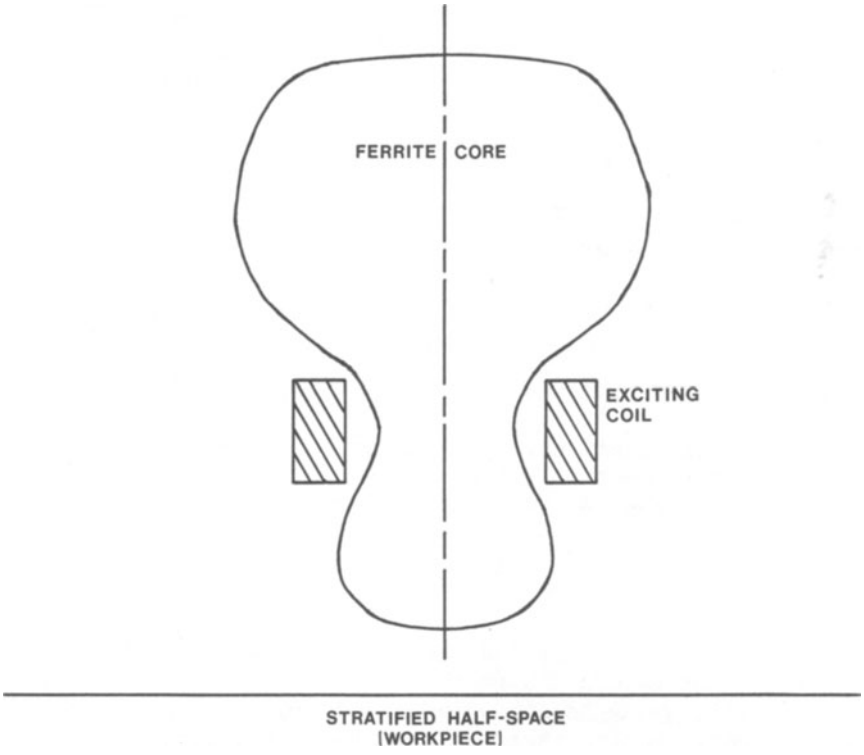

Figure 1. Ferrite core in the shape of a general body-of-revolution, with its exciting coil, in the presence of a stratified half-space workpiece.

NDE work, whereas the truncated cylinder of Figure 3 is used in high-frequency work. Again, the problems posed by Figures 2 and 3 possess an axis of rotational symmetry.

If the excitation of the ferrite is weak then the problem may be treated as linear, which means, among other things, that there will be no harmonic distortion of single-frequency sinusoidal signals. At the outset of this investigation we make the small-signal, linearized assumption, but we intend to lay out the appropriate paths to follow in dealing with the more general nonlinear problem.

Cores that are made from powdered ferrite materials are isotropic, but those made from single crystal ferrites are anisotropic. The mathematical approach that we use in developing the model will be sufficiently general that it could include anisotropic core materials, as well.

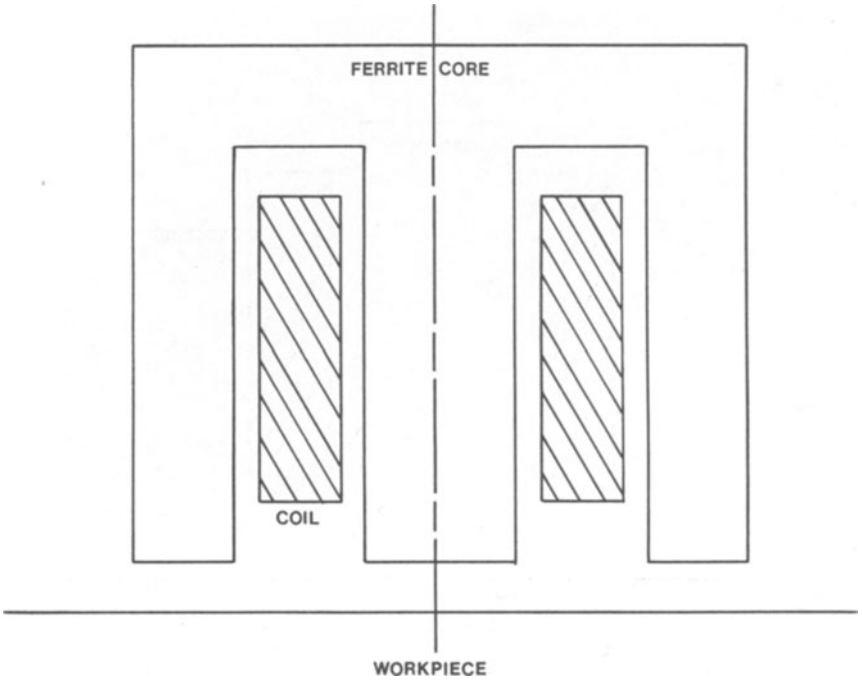

Figure 2. E-shaped body-of-revolution with exciting coil.

The problem solved by Dodd, et al. [1-3] differs from ours in that the ferrite core is absent. Thus, in the problem they solved the excitation source was also parallel to the workpiece (i.e., there was no irregularly shaped core to destroy the plane-parallel symmetry) and this permitted them to solve analytically a number of important problems. We can follow their analytical approach only so far (that point being the determination of a Green's function), and then we must continue with a numerical approach in order to compute the magnetization within the ferrite core. Having computed the core magnetization, we can compute the fields within the workpiece analytically, as well as the driving-point impedance of the coil/core combination.

In a sense, Dodd et al.'s work brought eddy-current NDE "of age" by showing how one could get useful analytical results based on a rigorous application of electromagnetic field theory. In this paper we extend the application of electromagnetic field theory to include numerical techniques for analyzing the fields produced by complex structures. Our approach is very much in the spirit of contemporary research in problem-solving in electromagnetics [4,5].

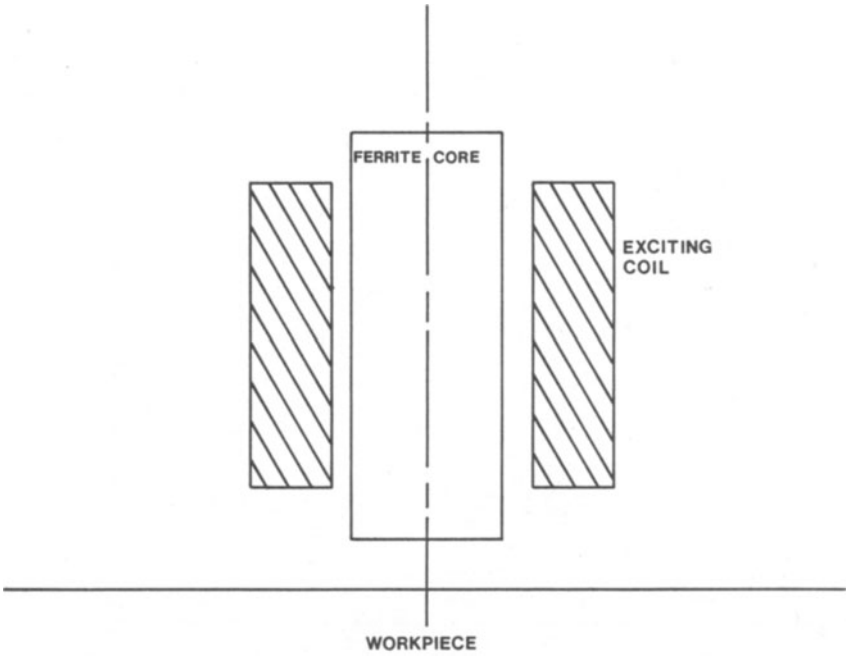

Figure 3. Truncated cylinder with exciting coil.

We start by replacing the ferrite core by an equivalent controlled source of Amperian currents, which, together with the true current in the exciting coil, comprise the total source of the electromagnetic field. The field is expressed as an integral over the regions occupied by the source currents, i.e., the core and coil. The integrand is a vector function of two arguments, one the source point occupied by the currents, and the other argument being the field point at which the electromagnetic field is to be evaluated. The Green's function computed by Dodd, et al., makes its appearance in this integral expression.

The controlled Amperian source current density is not known a priori, however, because it depends on the value of the field at the source point. Hence, we end up with an equation whose unknown appears both outside and inside an integral operator--an integral equation for the unknown Amperian source current density (which is directly related to the magnetization of the ferrite core). This integral equation is reduced to an algebraic system by the method of moments [6], and is then solved using a linear equation solver. Having the Amperian and true currents, we can compute the electromagnetic field at any point of space, including within the workpiece, by straightforward integration. The derivation of the integral equation and other analytical matters are the subject of [7].

ANALYSIS

Application of the vector Green's identity to Maxwell's equations in the sinusoidal steady-state leads to the volume integral equation for the magnetic field, $\bar{B}$:

$$\bar{B}(r,z) = B^{(i)}(r,z) + 2\pi \nabla \times \bar{a}_\phi \iint_{\text{core}} (1 - \frac{\mu_0}{\mu}) \bar{B}(r',z') \cdot \nabla' \times \bar{G}_{11}(r,z;r',z') r' dr' dz' \quad . \tag{1}$$

The first term is the incident field due to the coil, and the second is the field due to the induced magnetization, $\bar{M}$, where

$$\bar{M} = \bar{B}/\mu_0 - \bar{H} = \bar{B}(\frac{1}{\mu_0} - \frac{1}{\mu}), \tag{2}$$

and μ is the permeability of the ferrite. In (1) the subscripts on the Green's function, $\bar{G}$, correspond to the two regions of space: region 1 is the half-space above the workpiece, and region 2 is the workpiece. The first subscript locates the region in which the field point (r,z), resides, and the second the region in which the source point, (r', z'), resides. The derivation of $\bar{G}_{11}$ is given in [7].

The starting point in the numerical reduction of (1) is to partition the core in a regular grid. Based on this partition, we expand the unknown field in pulse functions

$$\bar{B}(r,z) = \sum_{j=1}^{N_c} \bar{B}_j P_j(r,z), \tag{3}$$

or in component form

$$B_r(r,z) = \sum_{j=1}^{N_c} b_j^{(r)} (\frac{r}{r_b}) P_j(r,z) \tag{4a}$$

$$B_z(r,z) = \sum_{j=1}^{N_c} b_j^{(z)} P_j(r,z) \ , \tag{4b}$$

where $\{b^{(r)}\}$, $\{b_j^{(z)}\}$ are the expansion coefficients for the r- and z-components, N_c is the number of cells in the grid and $P_j(r,z)$ is the jth pulse function, which is defined by

$$P_j(r,z) = 1, \quad (r,z) \text{ in jth cell} \tag{5}$$

$$= 0, \quad \text{otherwise.}$$

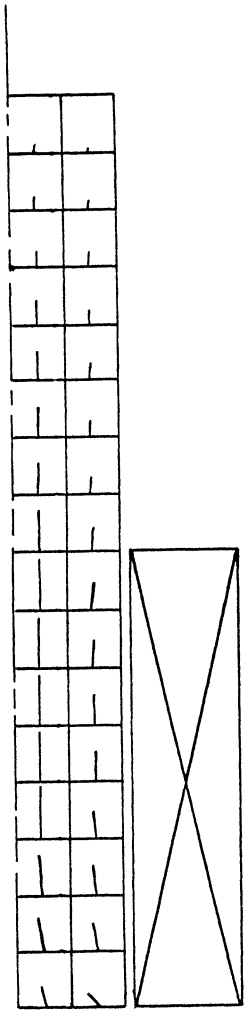

Fig. 4. Approximate $\bar{B}$-field within the cylindrical core.

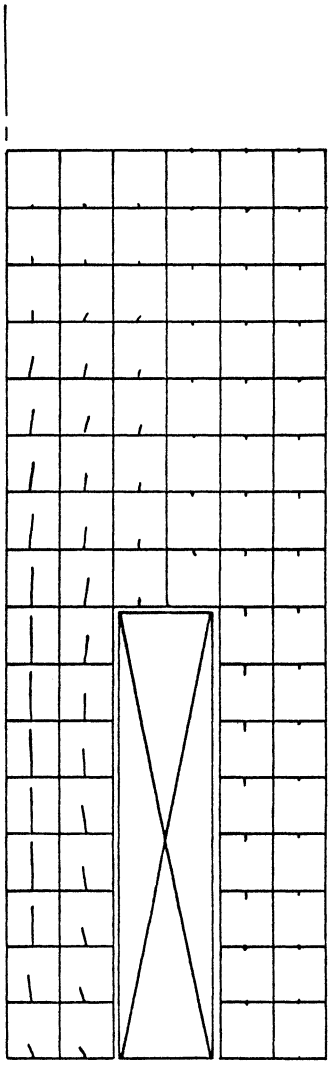

Fig. 5. Approximate $\bar{B}$-field within the E-shaped core.

Application of the Galerkin variant of the method of moments leads to the reduction of (1) to the vector-matrix equation:

$$\left[\begin{array}{c|c} A^{(rr)} - G^{(rr)} & -G^{(rz)} \\ \hline -G^{(zr)} & A^{(zz)} - G^{(zz)} \end{array}\right] \left[\begin{array}{c} b^{(r)} \\ \hline b^{(z)} \end{array}\right] = \left[\begin{array}{c} F^{(r)} \\ \hline F^{(z)} \end{array}\right] \tag{6}$$

The overall system-matrix is of order $2N_c \times 2N_c$.

Expressions for the matrix elements and forcing-function components of this linear system can be found in [7], together with a discussion of the numerical computation of the resulting infinite integrals.

RESULTS

After (6) is solved for the expansion coefficients, $\{b^{(r)}\}$, $\{b^{(z)}\}$, the results are then substituted into (4) to produce the components of the induction field, $\bar{B}$, within the core. With this field in hand it is possible to compute other functions. In this section we illustrate some of the results that have been obtained for the E-shaped and cylindrical cores. Some of the results correspond to the workpiece being absent, in which case $\{b^{(r)}\}$ and $\{b^{(z)}\}$ are real. When the workpiece is present $\{b^{(r)}\}$ and $\{b^{(z)}\}$ are complex.

Approximate $\bar{B}$-field Within the Core

Figure 4 shows the approximate $\bar{B}$-field within the cylindrical core, and Figure 5 shows the same thing for the E-shaped core, both when the workpiece is absent. In each case the line segments represent the approximate field at the center of each cell of the grid that was used in the method of moments. The line segments are shown emanating from the bottom or top line of a cell simply to facilitate the presentation.

The radius of the cylinder is 0.0625" and the height is 0.500". The inner radius of the coil is also 0.0625", the outer radius, 0.125", and the height is 0.250". The outer radius of the E-shaped core is 0.1875", and the height is 0.500". The same coil is used with the E-shaped core as with the cylinder. The permeability of the core is $1000\,\mu_0$.

We note that $\bar{B}$ is generally smaller in magnitude for larger radii. This means that, because the cross-sectional areas increase with increasing radius, the net magnetic flux entering the region is equal to the net flux leaving, as is to be expected from the condition $\nabla \cdot \bar{B} = 0$. Indeed, we have computed an approximate value of $\nabla \cdot \bar{B}$ at one point within the cylindrical core and have found it to be zero, certainly within the accuracy of the expansion in pulse functions. This is a very desirable feature of our results; it shows that the model produces physically consistent and accurate results with the grids shown.

Driving-point Impedance of the Coil and Core

The driving-point impedance of the coil is defined to be the ratio of the coil's induced voltage to its current. If the coil is uniformly and densely wound with n_c turns per unit area and occupies the region $r_1 \leq r \leq r_2$, $z_1 \leq z \leq z_2$, then the induced voltage is given by

$$V = j\omega(2\pi)^2 n_c^2 I\mu_0 \int_{r_1}^{r_2} rdr \int_{z_1}^{z_2} dz \int_{r_1}^{r_2} r'dr' \int_{z_1}^{z_2} dz' G_{11}(r,z;\, r',\, z')$$

$$+ j\omega(2\pi)^2 n_c \int_{r_1}^{r_2} rdr \int_{z_1}^{z_2} dz \iint_{\text{core}} (1 - \frac{\mu_0}{\mu})\bar{B}(r',z') \cdot$$

$$\nabla' \times \bar{G}_{11}(r,z;\, r',z')\, r'dr'dz'. \qquad (7)$$

The first term on the right-hand side of (7) is the voltage that is induced into the coil in the absence of the core (the coil self-voltage), and the second term is the additional voltage induced into the coil due to the induced magnetization within the core.

We have computed the driving-point impedance at the frequencies 1kHz, 10kHz, 100kHz, and 1MHz, and have presented the results in the impedance-plane plot of Figure 6. Here the real and imaginary parts of the driving-point impedance are displayed, with frequency as a parameter. The three curves correspond to the coil alone, coil+cylindrical core, and coil+E-shaped core, each in the presence of the workpiece. The interpretation of the diagram is that the coupling to the workpiece becomes tighter in going from the coil alone to the coil+E-shaped core.

The reactive part of the driving-point impedance is due partly to the self-inductance of the coil+core combination (as if the workpiece were absent) and partly to mutual interaction of the induced eddy currents within the workpiece. The resistive part of the impedance is due entirely to the effects of the induced eddy currents. At higher frequencies the eddy currents reside nearer the surface of the workpiece, due to the skin effect, therefore making the volume of interaction within the workpiece smaller. This means that the volume losses within the workpiece decrease, thereby decreasing the effective resistance of the workpiece, making the driving-point impedance of the coil+core combination reactive.

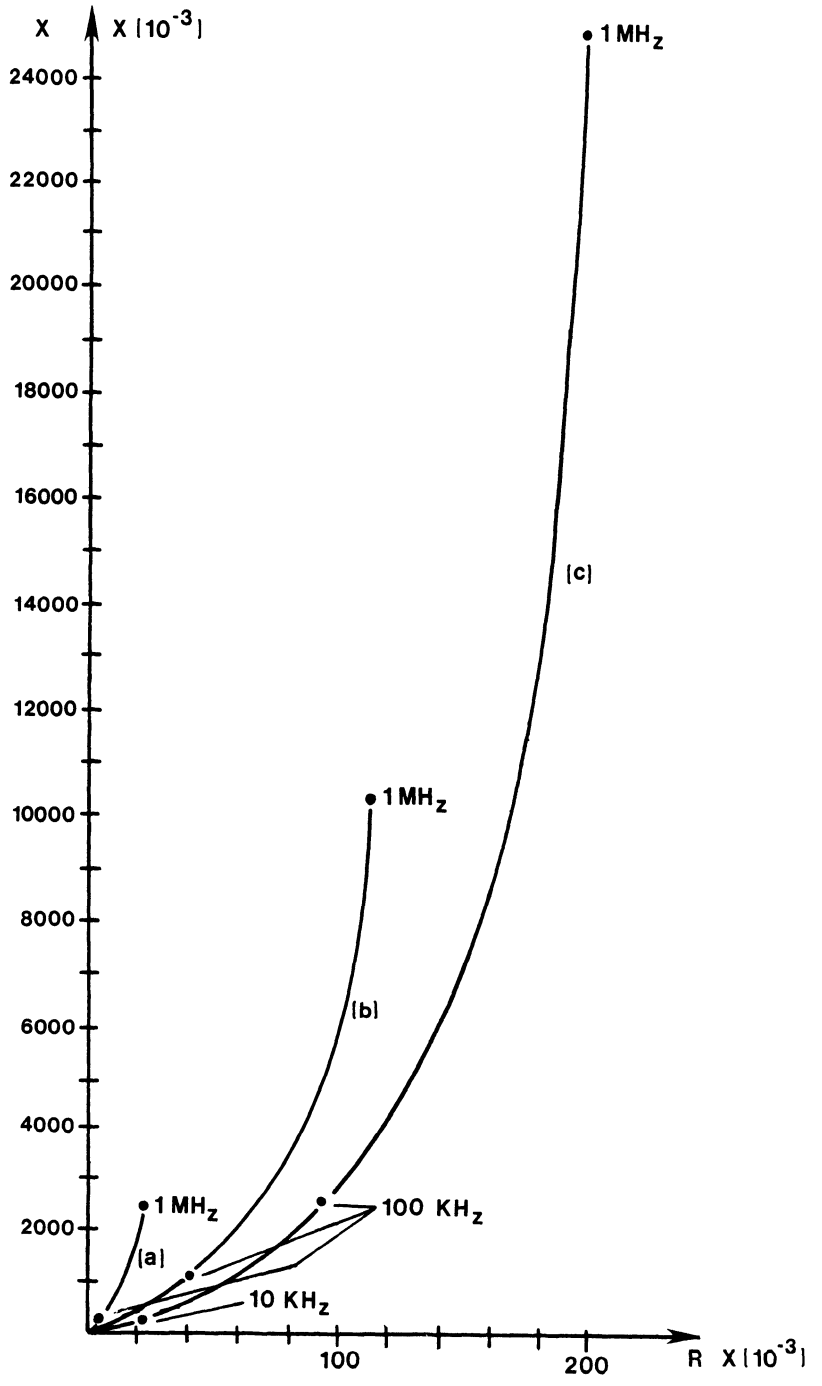

Figure 6. Impedance-plane plot of driving-point impedance. (a) coil alone, (b) coil + cylindrical core, (c) coil + E-shaped core.

Induced Fields Within the Workpiece

The purpose of the probe coil is to induce eddy currents within the workpiece. It is a fairly straight-forward computation to determine the distribution of induced eddy currents, once the induced magnetization within the core is known. The fundamental relation is

$$\bar{J}_2(r,z) = \sigma\bar{E}_2(r,z) = -j\omega\sigma\bar{A}_2(r,z) \quad , \tag{8}$$

where the subscript "2" denotes region 2, the workpiece, and σ is the conductivity of the workpiece. Hence, our first job is to determine an integral expression for $A_2(r,z)$ in terms of the current and magnetization in region 1, where the coil and core are located. The details are given in [7]; the result is

$$A_2(r',z') = 2\pi\mu_0 \iint_{\text{coil}} G_{21}(r',z';\, r,z)J(r,z)\,r\,dr\,dz + 2\pi\mu_0 \iint_{\text{core}} \nabla \times \bar{M}(r,z) \cdot \bar{G}_{21}(r',z';\, r,z)\,r\,dr\,dz \; . \tag{9}$$

The induced magnetization is determined by substituting (4) into (2). When this is done we can calculate the induced current density at any point within the workpiece from (8) and (9), for either core shape, or for the coil, alone. In Figure 7 we show the real (R) and imaginary (I) components of the current density induced at the surface of the workpiece, as a function of radial position. The frequency is 1 kHz. It is interesting to note that at this frequency the imaginary component dominates the real. A more important observation is that the E-shaped core+coil combination produces an intense, but localized, current distribution, and that in the vicinity of the maximum radial extent of the core the current density falls to zero. This is due to the fact that the net magnetic flux that is linked by a circular path beyond this radius is practically zero, because virtually all of the flux leaving the outer leg returns through the middle leg.

The current density induced by the cylindrical core, on the other hand, though somewhat larger than that produced by the E-shaped core, is much less localized. This is due to the fact that there is considerably more "leakage flux" produced by the cylindrical core (because it has no return path), than by the E-shaped core.

These results continue to hold at 1MHz (see Figure 8), except that at this frequency the real and imaginary components are practically equal. The bumpy nature of the curves for the cylinder and E-shaped cores is probably due to the discretization of the core in the numerical solution. We are investigating ways to smooth out these effects.

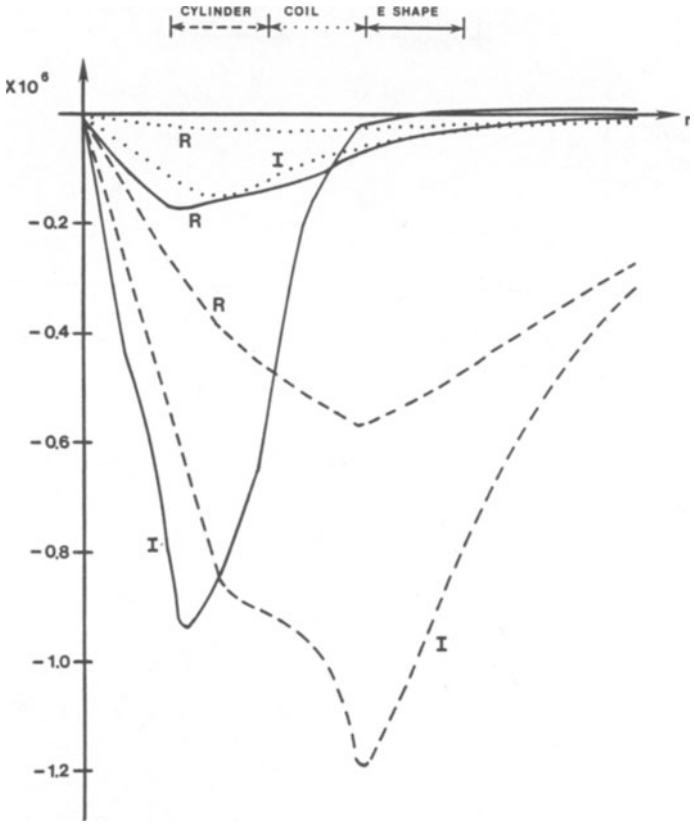

Figure 7. Induced eddy-currents at surface of workpiece, at 1 kHz.

COMMENTS, EXTENSIONS AND CONCLUSIONS

The model that we have derived is useful for the analysis of probes with linear, isotropic ferrite cores. It can be extended to apply to the following problem areas, all of which are important in contemporary eddy-current NDE technology:

- Analyze probe coils with anisotropic (single crystal) cores
- Time-dependent (pulsed) eddy-current problems (linear core)
- Time-dependent (pulsed) eddy-current problems (nonlinear core)
- Optimization of probe coil design to satisfy simultaneous constraints on eddy-current distribution and driving-point impedance

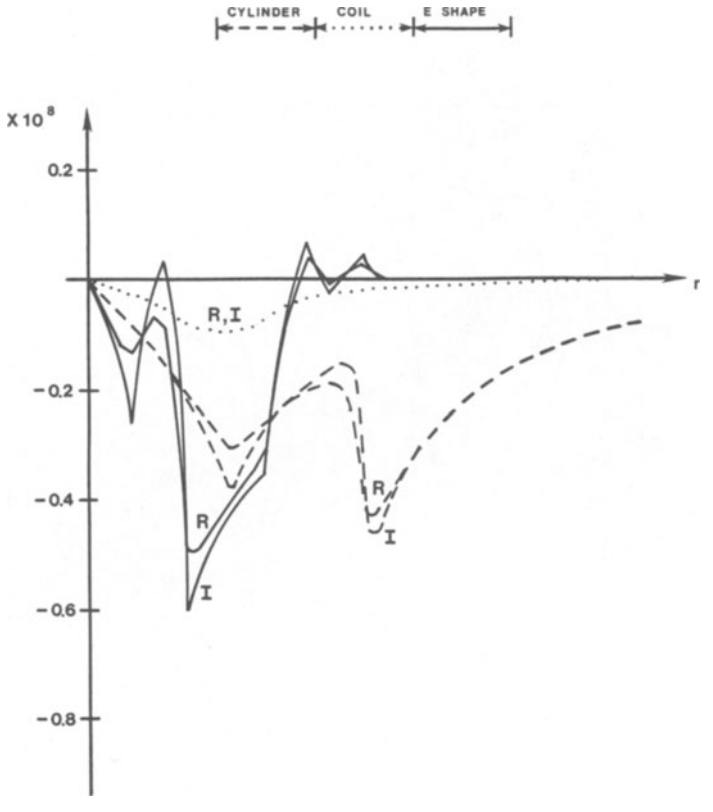

Figure 8. Induced eddy-currents at surface of workpiece, at 1 MHz.

All of these problems are solvable; they only require a sustained modeling effort. The rewards for such an effort could be immense in terms of improved design and understanding of probe coils with ferrite cores.

REFERENCES

[1] C. V. Dodd and W. E. Deeds, "Analytical Solutions to Eddy-Current Probe-Coil Problems," J. Appl. Phys., 39, 2829-2838 (1968).

[2] J. W. Luquire, W. E. Deeds, and C. V. Dodd, "Alternating Current Distribution Between Planar Conductors," J. Appl. Phys., 41, 3983-3991 (1970).

[3] C. C. Cheng, C. V. Dodd, and W. E. Deeds, "General Analysis of Probe Coils Near Stratified Conductors," Intern. J. Nondestructive Testing, 3, 109-130 (1971).

[4] R. Mittra, ed., Computer Techniques for Electromagnetics, New York, Pergamon Press, 1973.

[5] R. Mittra, ed., Numerical and Asymptotic Techniques in Electromagnetics, New York, Springer-Verlag, 1975.
[6] Roger F. Harrington, Field Computation by Moment Methods, New York, The Macmillan Company, 1968.
[7] Harold A. Sabbagh, "A Model of Eddy-Current Probes with Ferrite Cores," Final Report: Contract No. N60921-81-C-0076, with Naval Surface Weapons Center [Code R34], White Oak Labs, Silver Spring, MD 20910, 19 April 1982.

DISCUSSION

D.O. Thompson (Ames Laboratory): Did you make maps of the field in the work piece?

H.A. Sabbagh (Analytics): No, what I did was plot the current distribution. I thought that would probably be more useful than the B field or the A field, and the only current distribution I showed you was at the surface. I have done it in the report at 2.7mm, which is the skin depth of aluminum at 1 kHz, so you can see the skin effect, and in air you can quite dramatically see the effect of lift-off. The only thing I thought would be really useful would be the eddy current distribution, because that's ultimately what's doing the interrogating.

R.E. Beissner (Southwest Research Institute): Could you indicate how you would approach the time-dependent problem?

H.A. Sabbagh: There are two ways of doing this in modern numerical electromagnetics. One is to do what I've done for a sequence of frequencies: You do the inversion, you have a matrix inversion at each frequency, and you do it for 32 or 64 frequencies, and you use either an FFT (fast Fourier transform inversion) or, if you want to do initial value problems, you have to use the Laplace transform. And then you take both of those inverse transforms numerically, either via the FFT or via numerical inversionable Laplace transforms. The second way to do it, and a very elegant way but there are certain trade-offs, is to use what is known as the time-dependent integral equation. All the electromagnetics people do that problem, principally for interrogating aircraft in free space. They don't have a work piece. The presence of the work piece would be a real hindrance to the time-dependent integral equation, so my preference at the outset would be to take several frequencies. It will take many hours to generate that because at each stage, you have to do a matrix inversion, and then take an FFT. What I really need is some experimental verifications to make sure that my inductance values are correct, because I have no idea.